



A high-performance gel polymer electrolyte based on poly(vinylidene fluoride)/thermoplastic polyurethane/poly(propylene carbonate) for lithium-ion batteries

JIANGLAN XU, YUEWEN LIU, QI CAO*, BO JING, XIANYOU WANG and LI TAN

College of Chemistry, Xiangtan University, Xiangtan 411105, Hunan Province, People's Republic of China
E-mail: wjcaoqi@163.com

MS received 16 January 2019; revised 14 March 2019; accepted 26 March 2019; published online 31 May 2019

Abstract. Fibrous membranes of composites of poly(vinylidene fluoride) (PVDF)/thermoplastic polyurethane (TPU)/poly(propylene carbonate) (PPC) are prepared with different concentrations by electrospinning method. The physical properties of the films are characterized, such as morphology, porosity, thermal stability and mechanical properties. After electrospun films with different concentrations are activated to gel polymer electrolyte (GPE), we test their electrochemical properties. The morphology and the thermal stability of the PVDF/TPU/PPC nanofibers (NFs) with a concentration of 12% are the best. It shows the high tensile strength of 9.9 MPa and the maximum elongation of 110.8%. The ionic conductivity of its corresponding GPE is as high as 5.32 mS cm^{-1} , and the electrochemical stability window is up to 5.4 V at room temperature. In addition, it shows a high initial charge capacity of 165.8 mAh g^{-1} and a high initial discharge capacity of 165.1 mAh g^{-1} . The excellent properties make the PVDF/TPU/PPC based GPE (12%) more suitable for lithium-ion batteries.

Keywords. Poly(vinylidene fluoride) (PVDF); thermoplastic polyurethane (TPU); poly(propylene carbonate) (PPC); electrospinning; gel polymer electrolyte (GPE).

1. Introduction

Lithium-ion battery (LIB) has been considered as a major energy storage device due to its high energy density, long cycle life, and minimal memory effect.^{1–6} However, the safety problems caused by the leakage and combustion of organic liquid electrolytes limit the largescale application of LIB. GPE has been considered as a promising alternative because of its thermal resistance, the dimension stability and compatibility with lithium electrodes.^{7–9} The technique of electrospinning is a governable, uncomplicated and efficient approach to produce GPE.

PVDF has good thermal stability, good mechanical properties and excellent electrochemical stability. The polymer chain of PVDF contains strong push electron group of $-\text{CF}_2$ and has a high dielectric constant ($\epsilon = 8.4$), so that the lithium salt in the electrolyte system is fully dissolved and the number of carriers is more.^{10,11} PVDF is a semi-crystalline

polymer with high crystallinity and small amorphous region, which leads to the limitation of Li^+ conduction. Therefore, the ionic conductivity of PVDF based electrolyte is not ideal.¹² Moreover, the fluorine atoms on polymer chains may react with negative lithium and lithium salts, resulting in poor performance and safety of batteries.¹³ Therefore, it is necessary to modify the PVDF based electrolyte. Currently, some research activities are based on copolymer like poly(vinylidene fluoride) (PVDF)/poly(methyl methacrylate) (PMMA), poly(vinylidene fluoride) (PVDF)/poly(ethylene oxide) (PEO), poly(vinylidene fluoride) (PVDF)/polyacrylonitrile (PAN) as GPE for lithium-ion batteries.^{14–22} The results show that the mechanical and electrochemical properties of the blend electrolytes have been improved correspondingly. PVDF, with the best comprehensive performance, is very suitable as matrix material of GPEs. TPU is a polymer with good mechanical properties. It is commonly used to improve the elongation at break of other materials. It is a typical block

*For correspondence

polymer that contains two phases in the molecule.^{23,24} The hard segment provides support function, so that it has good mechanical properties, such as tensile strength, wear resistance, high elasticity, etc.²⁵ The soft segment can dissolve the cations in the lithium salts and facilitate the transportation of ions. When it is mixed with PVDF, the amino group (–NH) in its molecular chain can form hydrogen bonds with fluorine atoms, which makes the two polymers better compatible. PPC, which when synthesized with carbon dioxide and propylene oxide, can effectively reduce CO₂ emissions and mitigate the greenhouse effect.^{26,27} It is completely biodegradable and is a good substrate material for the preparation of environment-friendly polymer electrolytes.^{28,29} PPC has a good structure that is similar to carbonate plasticizer, which makes it compatible with lithium salts and has a good interface effect with common electrodes.³⁰ In addition, the polar ester group in its main chain structure can effectively capture and store liquid electrolyte, so PPC often shows high electrolyte absorption. As an amorphous polymer with a low glass transition temperature (T_g), the advantages of the three are complementary to each other after blending PPC with PVDF and TPU. So, the T_g of the whole electrolyte system decreased and the amorphous area increased, where not only the electrical conductivity has improved by facilitating the conduction of Li⁺, but also the mechanical properties have improved. It can be predicted that the obtained GPEs will have superior performance and will be suitable for diaphragm materials of lithium-ion batteries.

Our group has done some research on studying the PVDF/TPU/PAN-based GPE for lithium-ion batteries.³¹ But poor compatibility between PAN-based GPE and lithium electrode leads to the poor electrochemical performance of batteries, especially cycle performance.³² This experiment is the first time when green environmental protection materials (PPC) were used in the ternary gel polymer electrolyte and the electrochemical performance of it is better than PVDF/TPU/PAN-based GPE. Therefore, PVDF/TPU/PPC based GPE is more suitable for lithium-ion batteries in the society that advocates green and environmental protection.

2. Experimental

2.1 Materials

PVdF (Kynar 760, from Arkema), TPU (1190A, from yantaiwanhua) and PPC (average $M_w = 120$ k, from Henan Tianguan, China) were dried under vacuum at 80 °C for 24 h before being used. A certain amount of LiPF₆ was dissolved in ethylene carbonate (EC)/dimethyl carbonate (DMC) (1/1, v/v)

to produce a 1.0 mol L⁻¹ electrolyte solution, which was purchased from Tinci Materials Technology Co., Ltd. Acetone and N, N-dimethylformamide (DMF) were analytical purity with no further treatment and they were purchased from Baishi Chemical Industry Co., Ltd.

2.2 Preparation of PVDF/TPU/PPC fibrous membranes

The electrospun PVdF/TPU/PPC fibrous composite membranes were prepared by the electrospinning technique as follows. Mixtures of PVdF, TPU and PPC (4:4:1, wt./wt./wt.) were dissolved in a mixed solvent of DMF/acetone (3:1, wt./wt.) and magnetically stirred at room temperature for 24 h at a concentration of 9 wt.%. Then 10 wt.%, 11 wt.%, 12 wt.% and 13 wt.% PVDF/TPU/PPC solutions were made respectively in the same way. After that, the resulting homogeneous mixture was transferred to a plastic syringe and electrospun on a spinning machine (KATO Tech. Co., Japan) at ambient atmosphere. A high voltage of 24 kV is maintained between the tip of the nozzle and the collector (aluminum foil) with a flow rate of 0.7 mL h⁻¹. The electrospun films were received on the collector plate, then dried under vacuum at 60 °C for 12 h to remove residual solvent and prevent the collapse of the fiber structure.

2.3 Preparation of gel polymer electrolytes

At room temperature, the dried PVDF/TPU/PPC nonwoven films were put into the liquid electrolyte solution of 1.0 mol L⁻¹ LiPF₆-EC/DMC in the glovebox to be active for an hour, which was filled with argon. The electrolyte solution was absorbed into the holes of the fiber film and the inside of the fiber, and took them out and wiped the membrane's surface by filter papers, then the gel polymer electrolytes were obtained.

2.4 Membrane characterization

The microstructure of the electrospun films was observed by SEM (Hitachi S-3500 N, Japan). The conductivity of the samples is poor. It is necessary to spray gold on the surface of the sample before testing in order to obtain a clear and high-quality surface morphology. DSC (NETZSCH DSC-200PC Instrument) measurements were carried out under the nitrogen atmosphere with a speed of 20 °C/min from 20 to 200 °C.

The crystallization melting temperature and glass transition temperature of electrospun membranes can be obtained by DSC test and the crystallinity of these can be calculated by the formula (1).

$$\chi_c = \frac{\Delta H_f}{\Delta H_f^* \phi} \quad (1)$$

where χ_c is the crystallinity, ΔH_f is the enthalpy of fusion of electrospun membranes, ΔH_f^* is the enthalpy of fusion for the

totally crystalline PVdF, 104.7 J g^{-1} , θ is the mass fraction of PVDF in ternary electrospun membranes.

The chemical structure of the non-woven films can be investigated by the FTIR spectra (Spectrum One, PerkinElmer Instruments). The thermal stability of the electrospun films was examined by using the thermogravimetric analysis (model TQAQ 50, TA Company, USA). Under a dry nitrogen atmosphere, the thermal analysis (TGA) method was carried out range from 30–800 °C at a scan rate of 20 °C/min. The dried electrospun film was cut into small fixed-size discs with a drill. The thickness and diameter of the electrospun film were measured. By immersing membranes into an n-butanol solution for 1 h, the porosity of them was calculated by the formula (2)

$$P = \frac{W_w - W_d}{\rho_b V_p} \times 100\% \quad (2)$$

Among them, P is the porosity of membranes, W_w and W_d represent the weights of the membranes before and after soaking the membranes in n-butanol solution, V_p is the volume of the membranes, and ρ_b is the density of the n-butanol. Then membranes were immersed into the LiPF₆-EC/DMC electrolyte, the absorption of the them was measured by weight gain and calculated by the formula (3).

$$\text{Uptake} = \frac{W - W_0}{W_0} \times 100\% \quad (3)$$

W and W_0 represent the weights of the wet and dry membranes, respectively. The ionic conductivity of the polymer films was conducted with SS/GPE/SS blocking cells by AC impedance measurement, and the electrochemical analyzer (Zahner Zennium) was employed with a frequency from 0.1 Hz to 1 MHz. The ionic conductivity could be calculated by the formula (4).

$$\sigma = \frac{h}{R_b S} \quad (4)$$

σ is the ionic conductivity, R_b is the bulk resistance, h and S are the thickness and area of the membrane, respectively.

2.5 Performance test of assembled batteries

Electrochemical stability was measured by the linear sweep voltammetry (LSV), using an electrochemical analyzer (Zahner Zennium) at a scanning rate of 5 mV s^{-1} with a potential range from 0V to 8V.

The cathode material was composed of LiFePO₄, conductive carbon, and poly(vinylidene fluoride) (PVdF) (8:1:1, wt./wt./wt.) with N-methyl-2-pyrrolidone (NMP). The cathode mixture was coated on aluminum foil using the doctor blade technique and dried at 60 °C for 24 h in vacuum for further use. The manufacture of test battery was carried out in a glovebox filling argon, the oxygen and moisture level were lower than 0.1 ppm. The charge-discharge cycling tests of the Li/GPEs/LiFePO₆ battery were conducted between 2.0 V and 4.2 V by the Neware battery testing system (model BTS-51,

Shenzhen, China), under various current densities of 0.1, 0.2, 0.5, 1.0, and 2.0 C at room temperature.

3. Results and Discussion

3.1 Morphology and structure

The SEM images of the electrospun films prepared by different concentrations (9 to 13 wt.%) of PVDF/TPU/PPC polymer solution are shown in Figure 1. In the electrospinning process, the main forces acting on the droplets are electric field force, surface tension and interfaces between different materials. There are many factors that influence the morphology and structure of the membranes, such as the distance between the nozzle tip and the collector, the concentration, the applied voltage, and the dielectric constant of the blend. In this work, the only difference is the concentration of the polymer solution.

As can be seen from Figure 1, all the five electrospun membranes show a three-dimensional network composed of nanofibers with random orientation, which lead to a porous structure. The porous structure in the membrane can improve the adsorption capacity of liquid electrolyte and provide a way for the rapid migration of lithium ions. The appearance of electrospun membranes with a concentration of 9% is the worst. The fibers are uneven in size and diameter distribution. There are some beads in the fibers. This is due to the low viscosity of the spinning solution. The lower the viscosity of the solution is, the lower the surface tension is. Under the action of high voltage electric field, some droplets of polymer down before they become filamentous fibers completely, so the fibers of the electrospun film (9 wt.%) are mixed with many beads. The electrospun film (10 wt.%) has a slightly better surface morphology than that with 9% concentration. There are no beads in fibers, and the diameter distribution of the fibers is relatively uniform. The largest diameter of the fibers is 370 nm, the smallest diameter of the fibers is 110 nm, and the average diameter of the fibers is 210 nm. The average fiber diameter of 11% electrospun films is the smallest of all samples, about 200 nm. However, the arrangement of the fibers is as disorderly as the first two films, and the distribution of the fibers is not uniform. The PVDF/TPU/PPC NFs with a concentration of 12% is relatively uniform and slender, the average diameter is about 300 nm, and meanwhile, the distribution is very concentrated. The NFs with a concentration of 13% have good morphology and structure. The fibers themselves are uniform in thickness, regular in the arrangement and narrow

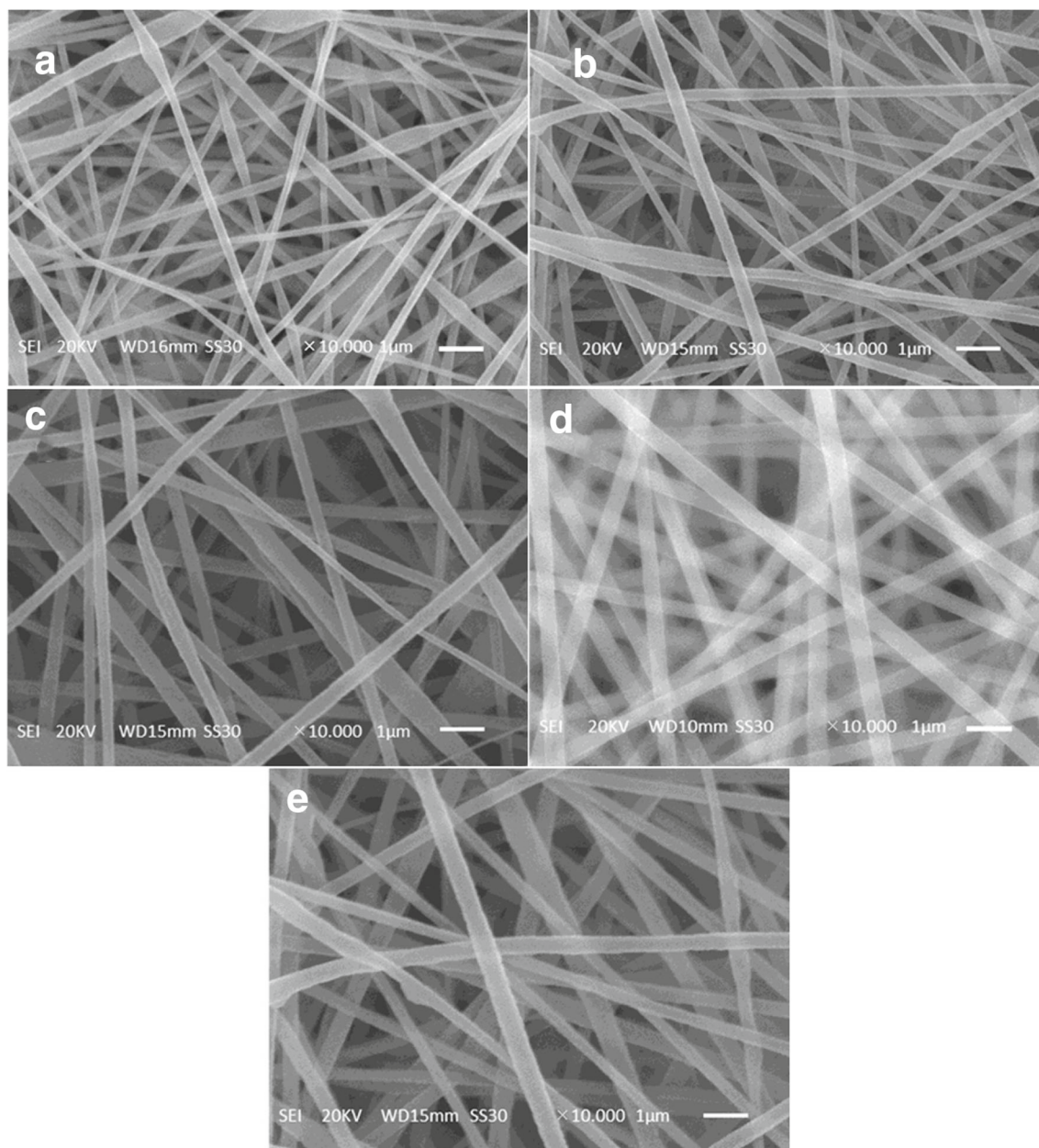


Figure 1. SEM images of PVDF/TPU/PPC electrospun membranes (a) 9%, (b) 10%, (c) 11%, (d) 12%, (e) 13%.

in diameter distribution. However, it can be clearly seen that the electrospun fibers with a concentration of 13% are thicker, and the average diameter of the fibers is the largest of the five kinds of films, about 360 nm. When the concentration of solution increases, the electric field force is not enough to overcome the increasing surface tension. The ability of droplets to be stretched into fibers decreases and the diameter of fibers (13 wt.%) increases accordingly. The diameter of the five kinds of films are shown in Table S3, Supplementary Information. The structure impacts the properties. So it can be inferred that the electrospun membranes (12 wt.%) have the best mechanical and electrochemical properties.

3.2 DSC analysis

The DSC analysis curves of the electrospun membranes prepared of different concentrations (9 to 13 wt.%) of PVDF/TPU/PPC polymer solution are shown in Figure 2, and thermodynamic properties of them were shown in Table 1. The enthalpy values of Table 1 are calculated by the integral area of the crystallization peak in Figure 2. The corresponding melting enthalpy can be obtained by integrating the area of the crystallization peak of the electrospun films. As shown in Figure 2, when the concentration of the spinning solution increases from 9% to 12%, the area of the corresponding crystallization peak decreases gradually,

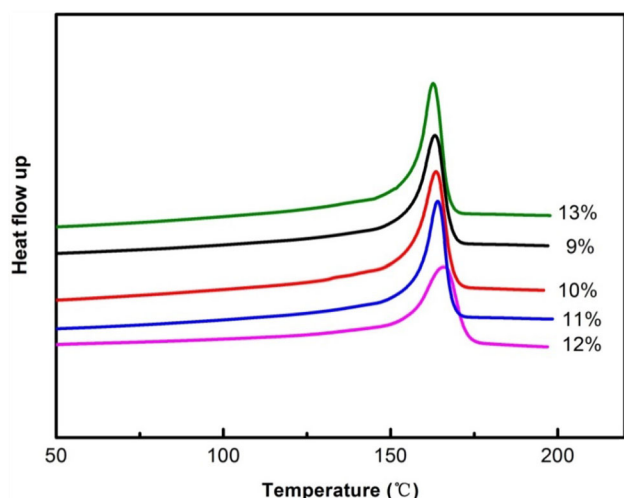


Figure 2. DSC thermograms of different concentration of PVDF/TPU/PPC.

Table 1. Thermodynamic properties of different concentration of TPU/PVDF/PS.

Sample	ΔH_f (J/g)	Crystallinity X_c (%)
PVDF/TPU/PPC (9 wt.%)	18.22	17.4
PVDF/TPU/PPC (10 wt.%)	17.67	16.9
PVDF/TPU/PPC (11 wt.%)	16.92	16.2
PVDF/TPU/PPC (12 wt.%)	14.55	13.9
PVDF/TPU/PPC (13 wt.%)	19.30	18.4

so the value of melting enthalpy and the crystallinity of the obtained electrospun film decreases gradually. When the concentration increases to 13%, the area of the crystallization peak increases and the crystallinity of the films increases. Therefore, 12% of the electrospun membranes have the smallest crystallinity (13.9%). The crystallinity can affect the ionic conductivity of the polymer. The lower the crystallinity of the film, the more free space is available for lithium ion migration. It can be inferred that the electrospun membranes (12 wt.%) have the highest ionic conductivity.

3.3 Mechanical property test

Figure 3 shows the stress-strain curves of PVDF/TPU/PPC based electrospun nanofibers with different concentrations and the mechanical properties of them were shown in Table S1, Supplementary Information. In this test, all the electrospun films were cut into 7 cm long strips with a thickness of 150 nm. It is found that the tensile strength of the NFs based on PVDF/TPU/PPC (12 wt.%) is 9.9 MPa and the elongation at break of it is 110.8% from the chart. To sum up, the PAN/TPU/PS

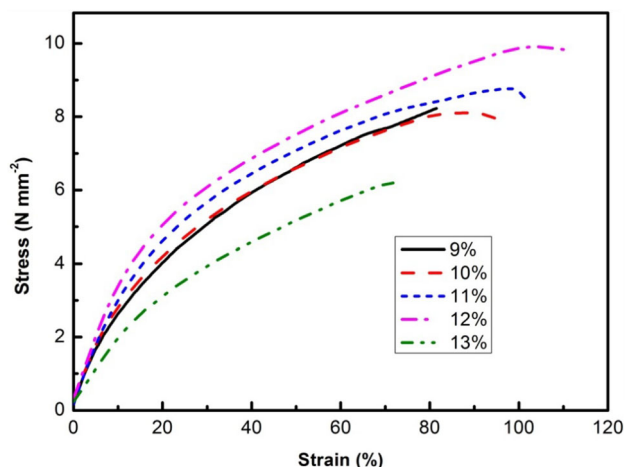


Figure 3. Stress-strain curves of different concentrations of electrospun PVDF/TPU/PPC membranes.

NFs with a concentration of 12% had the best mechanical properties. This is inseparable from its excellent fibre structure, which is consistent with the results of SEM analysis. Lithium dendrite is easily formed in the process of charging and discharging of metal lithium negative electrode, which pierces the battery separator and leads to a short circuit of the battery. The electrospun films (12%) have outstanding mechanical properties. When they are used as GPE in lithium-ion batteries, they have strong compression resistance and toughness, which can effectively prevent film perforation and short circuit of batteries, thereby improving the safety of batteries.

3.4 Porosity, electrolyte uptake, and ionic conductivity

Table S2 (Supplementary Information) shows the porosity for the PAN/TPU/PPC based fibrous polymer electrolyte, the specifications of the films used in the experiments are also detailed in this table. We can work out the porosity amount according to eq. (2). The porosity of the film depends on the diameter and density of the fiber. According to the data in Table S2 (Supplementary Information), the electrospun membrane with a concentration of 11%, with the smallest average fiber diameter, has the largest porosity (88%). The electrospun membrane with a concentration of 13%, with the largest average fiber diameter, has the smallest porosity (76%).

Figure S1 (Supplementary Information) shows the electrolyte uptake of PVDF/TPU/PPC based fiber membranes with different concentrations from 9% to 13%. We can work out the electrolyte uptake amount according to eq. (3). In two minutes, the absorption amount of the electrospun PVDF/TPU/PPC NFs with different

concentrations are 226% (9%), 258% (10%), 329% (11%), 362% (12%) and 185% (13%), respectively. After 20 min, the electrolyte absorption reaches saturation, and the absorption percentages of the electrospun NFs are 335% (9%), 379% (10%), 422% (11%), 449% (12%) and 319% (13%), respectively. The electrospun membrane (11%) has the largest porosity, but does not show the largest electrolyte uptake. Therefore, films with high porosity do not necessarily have high electrolyte uptake rate, and the electrolyte inside membrane with high porosity is easy to distribute unevenly and leakage,³³ so it is necessary for the film to have proper porosity.

The electrospun membranes with different concentrations were assembled into SS/GPE/SS blocking cells and tested for AC impedance at room temperature. The AC impedance spectra for the PVDF/TPU/PPC-based fibrous polymer electrolyte were shown in Figure 4. It is a typical AC impedance spectra for gel polymer electrolytes. In the range of test frequency, half-circle of atlas disappeared in the high-frequency region and presented a straight line. The intersection point between the straight line and the x-axis is the bulk resistance (R_b) of the gel polymer electrolyte.^{34–36} Ionic conductivity of

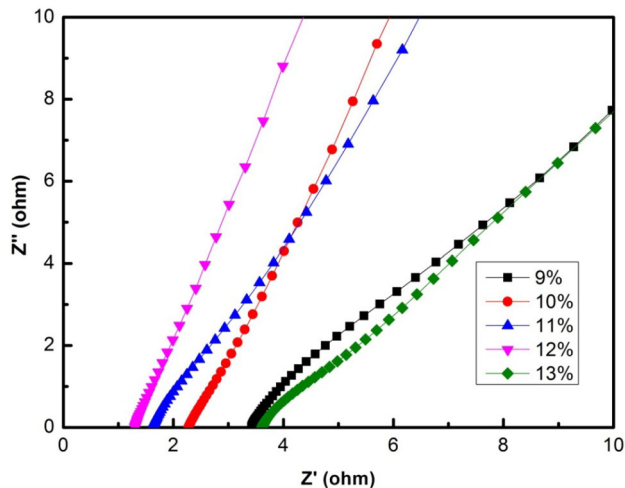


Figure 4. Impedance spectra of the PVDF/TPU/PPC based gel polymer electrolytes.

NFs were calculated by the formula (4) and the specifications of the films used in the experiments are also detailed in Table 2. The R_b values of PVDF/TPU/PPC GPEs with concentrations from 9% to 13% are 3.43 Ω , 2.28 Ω , 1.63 Ω , 1.31 Ω and 3.62 Ω . It can be seen from Table 2 that the ionic conductivity of GPE increases first and then decreases with the increase of concentration. When the concentration is 12%, the ionic conductivity of the GPE reaches the maximum (5.32 mS cm⁻¹) at the room temperature. This is consistent with the change trend of the electrolyte uptake rate. The more liquid electrolytes are absorbed, the greater the number of effective migration of Li⁺ is.³⁷ So, the ionic conductivity becomes greater. We can consider that 12% of PVDF/TPU/PPC blend solution is more suitable for the preparation of GPEs. Temperature can directly affect the concentration and the migration rate of charged particles. Figure S2 (Supplementary Information) shows the ionic conductivity of PVDF/TPU/PPC GPEs with concentrations of 12% at different temperatures (0 °C, 18 °C, 25 °C and 40 °C) and the specifications of the films used in the experiments are also detailed in Table S4 (Supplementary Information). It can be seen that the ionic conductivity of gel polymer electrolytes is directly proportional to the temperature. Because the higher the temperature is, the more charged the particles are, and the faster the migration rate of charged particles is.

3.5 Evaluation in Li/LiFePO₄ cells

Figure 5 shows the first charge-discharge capacity curves of cells assembled by PVDF/TPU/PPC based GPEs with different concentrations at room temperature at 0.1 C. It is observed that the charging voltage platforms of all GPE cells are about 3.45 V and the discharging voltage platforms are about 3.4 V. The small voltage difference between charge and discharge platforms indicates that there is good interface compatibility between PVDF/TPU/PPC based GPEs and electrode materials. The changing trend of charge-discharge capacity is consistent with that of ionic conductivity and electrolyte uptake. When the concentration of GPEs increases from 9% to 13%, the

Table 2. Ionic conductivity of the PVDF/TPU/PPC based gel polymer electrolytes.

Sample	Surface area (cm ²)	Thickness (cm)	R_b (Ω)	Ionic conductivity (mS cm ⁻¹)
PVDF/TPU/PPC (9 wt.%)	2.01	0.015	3.43	2.17
PVDF/TPU/PPC (10 wt.%)	2.01	0.015	2.28	3.27
PVDF/TPU/PPC (11 wt.%)	2.01	0.014	1.63	4.27
PVDF/TPU/PPC (12 wt.%)	2.01	0.014	1.31	5.32
PVDF/TPU/PPC (13 wt.%)	2.01	0.0155	3.62	2.13

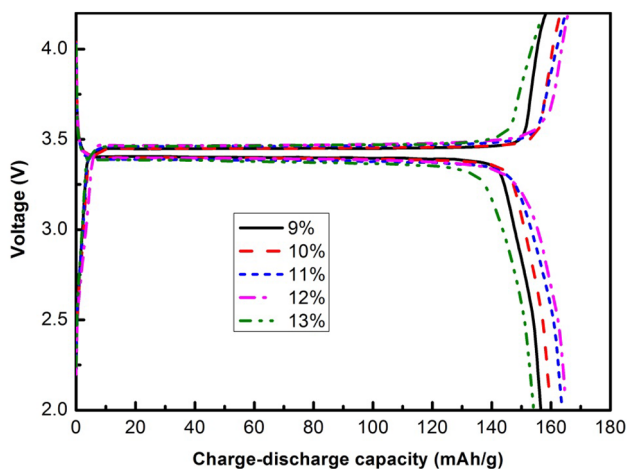


Figure 5. First charge-discharge capacities of different concentrations of GPEs based on electrospun PVDF/TPU/PPC membranes.

initial charge capacity of battery are 158.3 mAh g^{-1} , 163.2 mAh g^{-1} , 164.8 mAh g^{-1} , 165.8 mAh g^{-1} and 157.5 mAh g^{-1} , respectively. The first discharge capacity is 156.6 mAh g^{-1} , 159.8 mAh g^{-1} , 163.7 mAh g^{-1} , 165.1 mAh g^{-1} and 154.2 mAh g^{-1} , respectively. The first discharge capacity of cells, which were assembled by PVDF/TPU/PPC based GPEs with different concentrations, are more than 90% of the theoretical capacity of LiFePO_4 . Due to its good morphology, proper porosity, high electrolyte absorption and ionic conductivity, the GPE (12%) also exhibits very high charge-discharge capacity when assembled into cells.

The first charge-discharge capacity of the 12% GPE has been tested at different rates. As is shown in Figure 6, the charge capacity is 165.8 mAh g^{-1} and the discharge capacity is 165.1 mAh g^{-1} at 0.1C rate. The charge-discharge capacities are excellent, which is about 97.5% of the theoretical capacity of LiFePO_4 . At relatively larger rates of 0.2C, 0.5C and 1.0C, the charge capacities are $160.16 \text{ mAh g}^{-1}$, $154.75 \text{ mAh g}^{-1}$ and $145.53 \text{ mAh g}^{-1}$ and the discharge capacities are $159.34 \text{ mAh g}^{-1}$, $151.57 \text{ mAh g}^{-1}$ and $145.29 \text{ mAh g}^{-1}$. We all know that the degree of polarization is positively related to the current intensity. Therefore, different degrees of capacity attenuation of polymer batteries appear. The first charge-discharge capacities at high rate remain at a high level, which indicates that the GPEs based on electrospun PVDF/TPU/PPC membranes have excellent electrochemical performance.

Figure 7 shows a cycle performance diagram for cells at 0.1C rate. As can be seen from Figure 7, the cell, which assembled by PVDF/TPU/PPC based GPEs with different concentrations, all show good

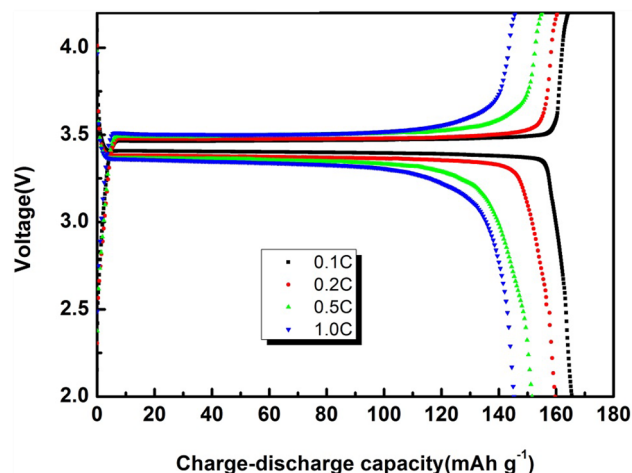


Figure 6. First charging and discharging curves of button cells at different rates.

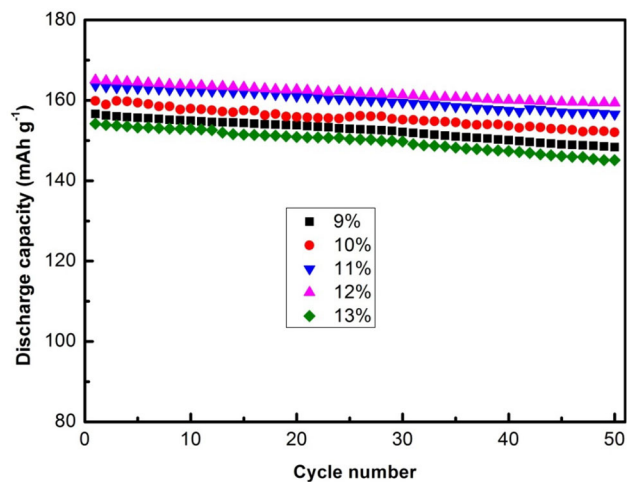


Figure 7. Cycle performance diagram of button batteries at a 0.1C rate.

cyclic stability. After 50 cycles, the discharge capacities were 148.4 mAh g^{-1} (9%), 152 mAh g^{-1} (10%), 156.6 mAh g^{-1} (11%), 159.4 mAh g^{-1} (12%) and 145.1 mAh g^{-1} (13%). The capacity retention rates of these batteries were 94.7%, 95.1%, 95.7%, 96.5% and 94.1%, respectively. The cell with GPE (12 wt.%) has the highest discharge capacity, and the process of charging and discharging is stable. The capacitance of GPE (12 wt.%) is not obviously attenuated and the capacity retention rate is 96.3%, so it shows its superior cycle performance.

Figure 8 shows a cycle performance and coulombic efficiency for the cell containing the PVDF/TPU/PPC based GPE (12 wt.%) at different rates. When the current densities are 0.1C, 0.2C, 0.5C and 1.0C, the first discharge capacities are 165.1 mAh g^{-1} , $155.30 \text{ mAh g}^{-1}$, $145.31 \text{ mAh g}^{-1}$ and $140.04 \text{ mAh g}^{-1}$, respectively. After 50 cycles, the discharge capacities are

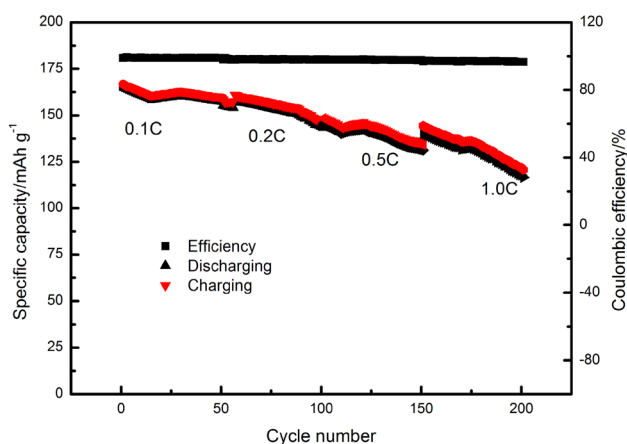


Figure 8. Cycle performance and Coulombic efficiency diagram of the button battery at different rates.

157.62 mAh g⁻¹, 143.48 mAh g⁻¹, 131.29 mAh g⁻¹ and 116.62 mAh g⁻¹, respectively. The capacity retention percentages are 95.47%, 92.4%, 90.4% and 83.3%, respectively. From the experimental results, we can see that the discharge capacities of the cells with PVDF/TPU/PPC based GPEs decreases as the rates increase, which is mainly attributed to the large current density and the increase of battery polarization. The volume of cathode materials will occur shrinkage and expansion in the process of charge and discharge. The larger the current density during the charge and discharge process, the greater the stress. Therefore, the particles of cathode material are more prone to rupture due to the rapid change in volume, which leads to faster cyclic decay. Their coulombic efficiencies (charge capacity/discharge capacity ratio) are basically above 96%, which meets the requirements of lithium-ion batteries.

3.6 Electrochemical stability

PVDF/TPU/PPC based GPEs with different concentrations were assembled into blocking batteries. The results of electrochemical stability tests of them by LSV are shown in Figure 9. Figure 9 depicts the way to find out the highest voltage of GPEs without electrochemical decomposition. From Figure 8, their electrochemical stability follows the order: 12%, 11% (5.4 V) > 10% (5.0 V) > 9%, 13% (4.9 V). Obviously, all electrospun films remain stable at the operating voltage (2.0–4.2 V) of lithium batteries. The electrochemical stability of GPE (11% and 12%) are the best, which may due to better compatibility with liquid electrolyte and NFs with less leakage of liquid electrolytes. Combining excellent physical and electrochemical properties of them, it can be concluded that the gel polymer electrolyte of

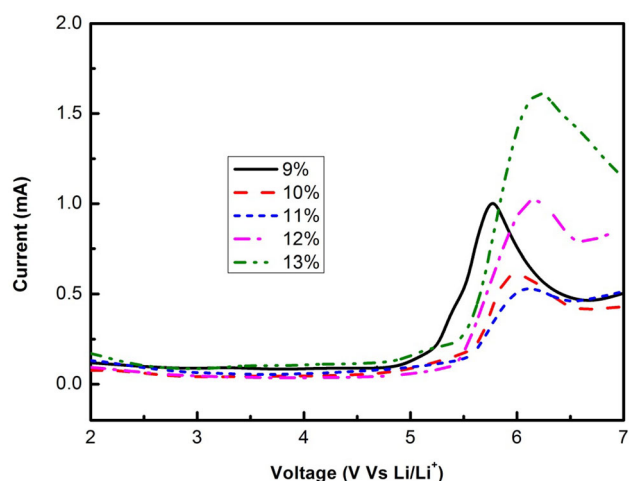


Figure 9. Linear sweep voltammograms of the gel polymer electrolytes.

PVDF/TPU/PPC (12 wt.%) is best for applications in a lithium-ion battery.

4. Conclusions

Five kinds of GPEs based on PVDF/TPU/PPC with different concentrations were prepared by the electrospinning technique in this research. It has been observed that the optimum concentration of novel high-performance PVDF/TPU/PPC-based gel polymer electrolyte is 12 wt.%. The PVDF/TPU/PPC (12 wt.%) based electrospun film owns the longest elongation at break of 110.8%, and it can bear the tensile strength of 9.9 MPa. Both the tensile strength and elongation at break are excellent. In addition, the electrospun membrane (12%) has the smallest crystallinity (13.9%) and high ionic conductivity of 5.32×10^{-3} S cm⁻¹ at room temperature. The first charge-discharge capacities of the cells with the PVDF/TPU/PPC (12 wt.%) based gel polymer electrolyte are about 165.8 mAh g⁻¹ and 165.1 mAh g⁻¹ at room temperature, and its capacity hardly drops after 50 cycles. The cells also show high discharge capacity retention percentage under the constant voltage conditions. The electrochemical stability of GPE (12%) has a wide electrochemical steady window so it can remain stable at the operating voltage (2.0–4.2 V) of lithium batteries. In conclusion, the PVDF/TPU/PPC (12 wt.%) based gel polymer electrolyte is very suitable for the diaphragm material of lithium-ion batteries.

Supplementary Information (SI)

Figures S1–S2 and Tables S1–S4 are available at www.ias.ac.in/chemsci.

Acknowledgements

The workers expressed their appreciation to the National Natural Science Foundation Youth Program (No. 51203131st).

References

1. Yu Y, Ji X B and Fan H J 2018 Post lithium ion batteries for emerging energy storage technologies *Green Energy Environ.* **3** 1
2. Tang Z Y 2017 Non-noble metal anode based dual-ion batteries: promising high-energy and low-cost energy storage devices *Sci. China Mater.* **60** 368
3. Yue Y and Liang H 2015 Hierarchical micro-architectures of electrodes for energy storage *J. Power Sources* **284** 435
4. Liu J Q, Wu X F, He J Y, Li J and Lai Y Q 2017 Preparation and performance of a novel gel polymer electrolyte based on poly(vinylidene fluoride)/graphene separator for lithium ion battery *Electrochim. Acta* **235** 500
5. Tarascon J-M and Armand M 2001 Issues and challenges facing rechargeable lithium batteries *Nature* **414** 359
6. Xiao L, Li Y W, Yi J-Y, Meng W, Deng B-H and Liu J-P 2018 Enhanced performance of solid-state Li-O₂ battery using a novel integrated architecture of gel polymer electrolyte and nanoarray cathode *Rare Met.* **37** 527
7. Cheng Q, Cui Z Y, Li J B, Qin S H, Yan F and Li J X 2014 Preparation and performance of polymer electrolyte based on poly(vinylidene fluoride)/polysulfone blend membrane via thermally induced phase separation process for lithium ion battery *J. Power Sources* **266** 401
8. Wienk I M, Boom R M, Beerlage M A M, Bulte A M W, Smolders C A and Strathmann H 1996 Recent advances in the formation of phase inversion membranes made from amorphous or semi-crystalline polymers *J. Membr. Sci.* **113** 361
9. Choi E-S and Lee S-Y 2011 Particle size-dependent, tunable porous structure of a SiO₂/poly(vinylidene fluoride-hexafluoropropylene)-coated poly(ethylene terephthalate) nonwoven composite separator for a lithium-ion battery *J. Mater. Chem.* **21** 14747
10. Fasciani C, Panero S and Hassoun J 2015 Novel configuration of poly(vinylidene fluoride)-based gel polymer electrolyte for application in lithium-ion batteries *J. Power Sources* **294** 180
11. Wu N, Cao Q and Wang X Y 2011 A novel high-performance gel polymer electrolyte membrane basing on electrospinning technique for lithium rechargeable batteries *J. Power Sources* **196** 8638
12. Horibe H and Taniyama M 2006 Poly(vinylidene fluoride) crystal structure of poly(vinylidene fluoride) and poly(methyl methacrylate) blend after annealing *J. Electrochem. Soc.* **153** 2347
13. Huang X Y, Zeng S S, Liu J J, He T, Sun L Y, Xu D H, Yu X Y, Luo Y, Zhou W Y and Wu J F 2015 High-performance electrospun poly(vinylidene fluoride)/poly(propylene carbonate) gel polymer electrolyte for lithium-ion batteries *J. Chem. Phys. C* **119** 27882
14. Nicotera I, Coppola L and Oliviero C 2006 Investigation of ionic conduction and mechanical properties of PMMA–PVdF blend-based polymer electrolytes *Solid State Ion.* **177** 581
15. Li Z, Wei J and Feng S 2008 PVDF/PMMA brushes membrane for lithium-ion rechargeable batteries prepared via preirradiation grafting technique *J. Polym. Sci. Part B: Polym. Phys.* **46** 751
16. Chiu F C and Yeh S C 2015 Comparison of PVDF/MWNT, PMMA/MWNT, and PVDF/PMMA/MWNT nanocomposites: MWNT dispersibility and thermal and rheological properties *Polym. Test.* **45** 114
17. Uludağ A A, Tokur M and Algul H 2016 High stable Li-air battery cells by using PEO and PVDF additives in the TEGDME/LiPF₆ electrolytes *Int. J. Hydrogen Energy* **41** 6954
18. Elashmawi I S, Elsayed N H and Altalhi F A 2014 The changes of spectroscopic, thermal and electrical properties of PVDF/PEO containing lithium nanoparticles *J. Alloys Compd.* **617** 877
19. Deng F L, Wang X E and He 2015 Microporous polymer electrolyte based on PVDF/PEO star polymer blends for lithium ion batteries *J. Membr. Sci.* **491** 82
20. Nthumbi R M, Adelodun A A and Ngila J C 2017 Electrospun and functionalized PVDF/PAN composite for the removal of trace metals in contaminated water *Phys. Chem. Earth Parts A/B/C* **100** 225
21. Wu Q Y, Liang H Q and Gu L 2016 PVDF/PAN blend separators via thermally induced phase separation for lithium ion batteries *Polymer* **107** 54
22. Zhu Y, Yin M and Liu H S 2017 Modification and characterization of electrospun poly(vinylidene fluoride)/poly(acrylonitrile) blend separator membranes *Compos. Part B* **112** 31
23. Vanheumen J D and Stevens J R 1995 The role of lithium salts in the conductivity and phase morphology of a thermoplastic polyurethane *ACS Pub.* **28** 4268
24. Kuo H-H, Chen W-C and Wen T C 2002 A novel composite gel polymer electrolyte for rechargeable lithium batteries *J. Power Sources* **110** 27
25. Wu N, Jing B, Cao Q and Wang X Y 2011 A novel electrospun TPU/PVdF porous fibrous polymer electrolyte for lithium ion batteries *J. Power Sources* **196** 8638
26. Zeng S, Wang S, Xiao M, Han D and Meng Y 2011 Preparation and properties of biodegradable blend containing poly(propylene carbonate) and starch acetate with different degrees of substitution carbohydrate *Polymers* **86** 1260
27. Du L, Qu B, Meng Y and Zhu Q 2006 Structural characterization and thermal and mechanical properties of poly(propylene carbonate)/MgAl-LDH exfoliation nanocomposite via solution intercalation *Compos. Sci. Technol.* **66** 913
28. Li X H, Meng Y Z, Wang S J, Rajulu A V and Tjong S C 2004 Completely biodegradable composites of poly(propylene carbonate) and short, lignocellulose fiber *Hildegardia populifolia J. Polym. Sci., Part B: Polym. Phys.* **42** 666

29. Shi X and Gan Z 2007 Preparation and characterization of poly(propylene carbonate)/montmorillonite nanocomposites by solution intercalation *Eur. Polym. J.* **43** 4852
30. Zhou D, Zhou R, Chen C, Yee W, Kong J, Ding G and Lu X 2013 Non-volatile polymer electrolyte based on poly(propylene carbonate), ionic liquid, and lithium perchlorate for electrochromic devices *J. Phys. Chem. B* **117** 7783
31. Liu Y W, Peng X X, Cao Q, Jing B, Wang X Y and Deng Y Y 2017 Gel polymer electrolyte based on poly(vinylidene fluoride)/thermoplastic polyurethane/polyacrylonitrile by the electrospinning technique *J. Phys. Chem. C* **121** 19140
32. Croce F, Gerace F, Dautzemberg G, Passerini S, Appetecchi G B and Scrosati B 1994 Synthesis and characterization of highly conducting gel electrolytes *Electrochim. Acta* **39** 2187
33. Huang X, Zeng S and Liu J 2015 High-performance electrospun poly(vinylidene fluoride)/poly(propylene carbonate) gel polymer electrolyte for lithium-ion batteries *J. Phys. Chem. C* **119** 27882
34. Pouyan S S, Gereon S and Dirk U S 2018 Non-invasive investigation of predominant processes in the impedance spectra of high energy lithium-ion batteries with Nickel-Cobalt-Aluminum cathodes *J. Power Sources* **406** 185
35. Balasundaram M, Vishwanathan R, Christopher Y and Palani B 2017 Investigation of physico-chemical processes in lithium-ion batteries by deconvolution of electrochemical impedance spectra *J. Power Sources* **361** 300
36. Macdonald J R 1974 Simplified impedance/frequency-response results for intrinsically conducting solids and liquids *J. Chem. Phys.* **61** 3977
37. Li L, Liu L, Qing Y, Zhang Z, Yan N and Wu Y 2018 Stretchable alkaline poly(acrylic acid) electrolyte with high ionic conductivity enhanced by cellulose nanofibrils *Electrochim. Acta* **270** 302